Investigation of the Temperature Homogeneity of Die Melt Flows in Polymer Extrusion

DOI:
10.1002/pen.23784

Document Version
Submitted manuscript

Investigation of the Temperature Homogeneity of Die Melt Flows in Polymer Extrusion

Chamil Abeykoon[1], Peter J. Martin[1], Adrian L. Kelly[2], Kang Li [3], Elaine C. Brown[2], Phil D. Coates[2]

[1]*School of Mechanical and Aerospace Engineering, Queen's University Belfast, Belfast, BT9 5AH, UK*

[2]*IRC in Polymer Science and Technology, School of Engineering, Design and Technology, University of Bradford, Bradford, BD7 1DP, UK*

[3]*School of Electronics, Electrical Engineering and Computer Science, Queen's University Belfast, Belfast, BT9 5AH, UK*

ABSTRACT

Polymer extrusion is fundamental to the processing of polymeric materials and melt flow temperature homogeneity is a major factor which influences product quality. Undesirable thermal conditions can cause problems such as melt degradation, dimensional instability, weaknesses in mechanical/optical/geometrical properties, etc. It has been revealed that melt temperature varies with time and with radial position across the die. However, the majority of polymer processes use only single point techniques whose thermal measurements are limited to the single point at which they are fixed. Therefore, it is impossible for such techniques to determine thermal homogeneity across the melt flow. In this work, an extensive investigation was carried out into melt flow thermal behavior of the output of a single extruder with different polymers and screw geometries over a wide range of processing conditions. Melt temperature profiles of the process output were observed using a thermocouple mesh placed in the flow and results confirmed that the melt flow thermal behavior is different at different radial positions. The uniformity of temperature across the melt flow deteriorated considerably with increase in screw rotational speed whilst it was also shown to be dependent upon process settings, screw geometry and material properties. Moreover, it appears that the effects of the material, machine and process settings on the quantity and quality of the process output are heavily coupled with each other and this may cause the process to be difficult to predict and variable in nature.

INTRODUCTION

Process thermal homogeneity and stability are major requirements for producing good quality products in any polymer process. Therefore, producers are very much interested in process thermal monitoring and control to minimize product defects, process down times, waste of material, energy, labor, etc. However, it is unlikely that existing industrial techniques can provide process thermal information to the required accuracy and detail and hence research is underway to improve thermal monitoring and control of polymer processing. Of the polymer processing techniques, extrusion is one of the most important as the majority of polymeric materials are processed though a screw extruder at least once prior to their final application [1]. If the process cannot be monitored accurately, thermal control cannot be fully achieved [2]. Therefore, accurate thermal monitoring is key to achieving the required level of process thermal stability, where stability is defined in terms of spatial and temporal thermal homogeneity rather than in reference to polymer degradation. It is obvious that process thermal control strategies are dependent on the accuracy and resolution of the associated temperature measurement techniques. Further development of extrusion process thermal monitoring and control could help to combat some of the major problems currently experienced by the industry such as long downtimes, waste of energy, labor and materials, high scrap rates, etc. Further details of the basic process mechanisms, process operation and functional requirements of polymer extrusion can be found in the literature [3, 4]. Some of the previous attempts made to investigate extrusion process thermal behavior are briefly discussed in the following section.

Thermal measurement techniques in polymer extrusion

Melt temperature measurement techniques applicable to polymer extrusion are outlined in this section. A comprehensive review of single point and bulk temperature measurement techniques used in research was previously presented by the authors together with their operating principles and an evaluation of several sensor types [4-6].

Wall mounted thermocouples (based on the thermoelectric effect) are the most commonly used melt temperature sensors in the polymer processing industry [7-10]. Two types of wall mounted thermocouples are commercially available which may be classified as non-insulated and insulated. The insulated thermocouple is equipped with internal insulation to limit the influence of metal barrel wall temperature on the measured value.

They are available with different probe arrangements including flush mounted, intrusive to melt flow by up to a few millimeters or with the facility of traversing into the melt flow manually/mechanically as shown in Figure 1.

The main advantages of wall mounted thermocouples are that they are easy to use, require little maintenance and are relatively inexpensive. However, despite insulation, the measurements are highly affected by the metal wall temperature and thermocouples are not capable of detecting rapid variations of the melt temperature due to their slow response time [3, 10, 11].

Infrared (IR) sensors can also be used for melt temperature measurement and several attempts have been made to monitor the bulk melt temperature during extrusion from IR measuring devices [10, 12-15]. It was found that an IR sensor can detect rapid variations in melt temperature, unlike wall mounted thermocouples, but that measurements were affected by material properties related to the emissivity of the melt, and therefore requires careful analysis.

Ultrasound techniques [16-22] use an ultrasonic probe together with associated pulser-receiver electronics for measurements which correlate the longitudinal ultrasonic wave velocity with the melt temperature. This technique has successfully been used to obtain bulk temperature across the flow and requires careful calibration but is highly accurate. Thermal imaging techniques have also been used in polymer extrusion [9, 23-25]. They are capable of providing excellent indications of temperature field, but are relatively expensive and not easily used for internal measurements. A technique based on the nuclear magnetic resonance (NMR) principle [26] and an electrical capacitance tomography (ECT) technique [27] have been proposed but these are still in an early stage of development. Both of these techniques have the advantage of being non-invasive but are complex and expensive, and the ECT technique requires an array of sensors.

Few studies have been reported on thermal profile measurement techniques in polymer extrusion. In early work [28-31], attempts were made to observe the radial melt temperature profile by fixing thermocouples along supporting frames or bars, but the techniques are invasive and subject to errors through conduction and the effects of shear heating. Pittman [32] has presented a finite element analysis to explore the errors in melt temperature measurement due to viscous heat generation and thermal interactions (e.g. conduction) between transducer and machine parts. Traversing thermocouple probes (i.e. similar to the arrangements D and E shown in Figure 1) were also used by several authors [10, 15, 33] to observe the melt temperature profile across the melt flow but these are similarly affected by shear heating and conduction errors in addition to disturbing the melt flow. A fluorescent measurement technique [34] has yielded useful data, but requires complex instrumentation and the need to dope polymers with temperature sensitive fluorescent dyes, making this a research tool rather than an option for most industrial processes. The thermocouple mesh used for this work has previously been described [35] and used to monitor melt temperature profiles [4-6, 33, 36-44] that illustrated the factors influencing the melt temperature homogeneity including process settings such as screw speed, barrel set temperatures, screw geometry and polymer properties. The meshes are constructed by thermocouple wires of small diameter (i.e. 0.3mm) and hence, although invasive, the melt flow is not significantly disturbed. However, careful attention is required in situations where the melt flow becomes highly viscous, for example at high throughputs where complete melting has not been achieved, as this may lead to damage of the thermocouple wires. The mesh was situated prior to die entry in a 174mm long adapter that was positioned between the barrel and the die. It was found for conventional single flighted screws that both spatial and temporal temperature variations increased as screw speed (throughput) increased and that the highest fluctuations existed a few millimeters away from the die wall. Barrel temperature changes were also shown to influence the profile to a lesser extent.

Melt flow thermal homogeneity

The main function of an extruder is to deliver a homogeneous polymer melt at a specified uniform temperature and pressure. Process output is required to be homogenous in composition, colour and temperature. To achieve this dominant requirement, extruders are generally equipped with an efficient drive and feed system, a screw designed to melt and convey the polymer and devices such as temperature and pressure transducers to monitor the system for troubleshooting and control. Additionally, devices such as mixers, gear pumps and controlled feeding devices may be used to improve the quality of melt output. Although, melt quality (defined as a thermally homogeneous melt at a constant throughput) is a key variable in polymer extrusion only a few thermal monitoring techniques are able to determine thermal stability and homogeneity across the melt flow cross-section in real-time. Therefore, extrusion processors may have limited understanding of the actual thermal behavior across the melt flow cross-section and maybe unaware of the effects of radial thermal fluctuations on their product quality and processing problems.

The aim of this work was to explore melt temperature homogeneity across a range of extrusion conditions to provide an improved understanding of the individual and combined effects of various processing conditions (such as screw geometry, material, and process settings) on thermal homogeneity. Four commonly used commercial thermoplastics and three different screw geometries were used for the experiments at five discrete screw speeds and three temperature settings. The study was focused on single screw extrusion and the experiments were performed to replicate industrial processing conditions by covering the full operating range of the extruder (i.e. 0-100rpm) using commercial grade polymeric materials.

EQUIPMENT

All measurements were carried out on a 63.5mm diameter (D) single screw extruder (Davis Standard BC-60). Three different screws were used for the tests: a gradual compression (GC) screw, a rapid compression (RC) screw, and a barrier flighted (BF) screw with a Maddock mixer. The geometrical details of the screws (i.e. compression ratio (CR) and length (L) of each section and channel heights (H) as functions of screw diameter) are given in Table 1.

The extruder was fitted with a 38mm diameter adaptor prior to a short cylindrical die with a 12mm bore. The extruder barrel has four separate temperature zones and another three separate temperature zones at the clamp ring, adapter and die. Each of these temperature zones is equipped with a separate temperature controller which allows individual control of the set temperature. The arrangement of the apparatus (i.e. extruder barrel, adapter and die) is shown in Figure 2. In all experiments, melt temperature profiles at the adepter (i.e. prior to entering the 12mm die) were measured using thermocouple meshes (TCM) placed in-between the adapter and die as shown in Figure 3. The details of the thermocouple meshes used are given in Table 2. The physical arrangement of the thermocouple mesh is shown in Figure 4.

As previously reported by Brown el al. [35] and Kelly et al. [37], die melt temperature measurements are symmetrical across the centerline of the thermocouple mesh when averaged over sufficient time. Therefore, the thermocouple junctions (i.e. between a number of positive wires and the negative wire) were placed asymmetrically across the melt flow along the diameter of the mesh as shown in Figure 4, and this asymmetric placement of wires gave the opportunity to increase the number of effective temperature measurements across the melt flow by mirroring them over the centerline to obtain the complete die melt temperature profile. Moreover, an insulated wall mounted thermocouple (0.5mm in diameter and flush mounted to the wall) was used to measure the temperature of the melt close to the die wall and this measurement was used as the melt temperatures of the ±19mm radial positions for generating the melt temperature profiles across the melt flow. A data acquisition programme developed in

LabVIEW was used to communicate between the experimental instruments and a PC. All signals were acquired at 10Hz using a 16-bit DAQ card (National Instruments (NI) PCI-6035E) through a thermocouple connector box (NI TC-2095) and a low-noise signal conditioning box (NI SCXI-1000).

MATERIALS & EXPERIMENTAL CONDITIONS

Four polymers were used for these experiments: a virgin high density polyethylene (HDPE), HM5411, from INEOS Olefins & Polymers; a recycled extrusion grade high density polyethylene (RHDPE), H-450, from Cherry Plastics Ltd; a virgin low density polyethylene (LDPE) LD150R, from Dow Plastics; and a virgin polypropylene (PP), 100-GA03, from INEOS Olefins & Polymers. More details on the properties of these materials are given in Table 3. Three different extruder temperature settings were selected as described in Table 4 and denoted as A (low temperature), B (medium temperature) and C (high temperature).

These settings were selected by considering the material properties and the screw geometry to achieve normal process operating conditions throughout the experiments while covering a wide operating window of the extruder. In this study, three different sets of experiments were carried out to identify the effects of the screw geometry (EXP-1), material (EXP-2) and set temperatures (EXP-3) on the melt flow temperature homogeneity. Further details of the conditions used in each experiment are given in Table 5.

Data were recorded continuously at a 10Hz sampling speed when applying step changes in screw speed. The overall time of the each test was around 45 minutes and the extruder was allowed to stabilize after each step change in screw speed. The average melt temperatures (i.e. T_{mean}) over the final minute at each screw speed were used to generate melt temperature profiles and the same set of data collected at the last minute at each screw speed was used for all the other evaluations.

RESULTS & DISCUSSION

Radial melt temperature profiles in the extruder die adapter generated from experimental measurements were observed to investigate the effects of screw geometry, material and set temperature on melt temperature homogeneity. These profiles at each screw speed were plotted by rotating the single measured axis around its centre point, and the corresponding profiles are shown in the following sections. All sub-figures are plotted over similar scales to clearly identify the individual effects, and color maps are provided to indicate the melt temperature levels/variations across each temperature profile. Also, sub-figures in each column of all the major figures are presented in the order of low speed to high speed from top to bottom.

Effects of screw geometry on melt flow temperature homogeneity

Three different experimental trials were carried out with the RC, GC and BF screws using LDPE to observe the effects of screw geometry on the temperature profile of the melt flow, with set conditions detailed EXP-1 in Table 5. Extruder temperatures were set to condition B during all the trials and the corresponding melt temperature profiles are shown in Figure 5. Figure legends are given at the top of each sub-figure in the format of screw geometry-screw speed (e.g. BF-10 refers to the barrier flighted screw at 10rpm). The three columns of Figure 5 from left to right show the melt temperature profiles with the BF, GC and RC screws respectively. Profile shapes and color distributions (relating to measured temperature across the melt flow) clearly show that spatial melt temperature homogeneity deteriorated as screw rotation speed increased. With increasing screw speed, a reduction in profile flatness and development of a peak in the centre of the melt flow was observed. The BF screw showed the flattest melt temperature profiles (indicating better thermal homogeneity) of all the three screws, and also showed the smallest variation in melt temperature with increasing screw speed. These data agree with a previous study by Kelly et al. [37, 44]. The separation of melt and solid in the BF screw and the spiral Maddock mixer at the end of the screw are thought to be responsible for the improved homogeneity [45]. Melt temperature profiles across the melt cross-section after the BF screw do not exhibit shoulder regions at 70rpm and 90rpm speeds unlike the profiles observed with the single flighted screws. Therefore, it is clear that screw geometry has a significant effect on the magnitude of spatial variations in the melt temperature. The minimum, mean and maximum melt temperatures achieved at each screw speed with the different screws are shown in Table 6.

Screw geometry was found to affect both the magnitude and distribution of the melt temperature across the flow. Of the three screws, the RC screw exhibited highest maximum melt temperature at 10rpm. Melt temperature with the GC screw was highest at speeds of 30rpm and 50rpm, while the melt temperature with the BF screw was highest at 70rpm and 90rpm. However, the GC screw showed highest mean melt temperature at 10 rpm, 30 rpm and 50 rpm, while the mean melt temperatures achieved by the BF screw were highest at 70 rpm and 90 rpm. The highest magnitude of variation in melt temperature (i.e. the difference between the highest and lowest melt temperatures) was observed with the GC screw at 90rpm with a value of 34.5^{o}C. As reported in the literature [46], the temperature of the screw has a considerable impact on the melting process. Although the same material and process settings were used in this experiment, the surface temperature of the screws may be variable since the mechanical heat generation is a function of screw geometry. However, screw temperature cannot be measured in this extruder arrangement. The rate of mass throughput (i.e. melting capacity) and the level of material mixing also depend on the screw geometry [47, 48] and will also impact upon the heat transfer and contribute to the measured melt temperature profiles.

Effects of material on melt flow temperature homogeneity

LDPE, HDPE and PP were processed to observe the effects of polymer type on the thermal homogeneity of extruder melt flow output at set temperature condition B (i.e. under the EXP-2, details given in Table 5). The BF screw was used in these experiments. Melt temperature profiles are shown in Figure 6. Figure legends included at the top of the each sub-figure are in the following format: material-screw speed (e.g. LDPE-10 means the LDPE material at 10rpm). The three columns of Figure 6 from left to right show melt temperature profiles with the LDPE, HDPE and PP materials, respectively. The minimum, mean and maximum melt temperatures achieved at each screw speed for different materials are given in Table 7.

No significant differences were observed in maximum melt temperature between the different materials at the same screw speed. However, it is apparent that the level of the mean melt temperature (i.e. the highest for PP at 10 rpm, 50 rpm, 70 rpm and 90 rpm while at 30 rpm the highest for HDPE) depended on the material to some extent. Of these three materials, PP showed the highest maximum melt temperature at screw speeds of 10rpm, 30rpm and 50rpm, but the HDPE temperatures were highest at 70rpm and 90rpm. In addition, PP showed the lowest minimum melt temperature at 90rpm although its temperature was highest at low screw speeds. As the same screw geometry and barrel set temperatures were used to process all the materials, the significance of differences in the rheological and thermal properties of each material is clear. Additionally, it has been reported that resin form (e.g. pellets, flakes, power) and pellet shape/size can also affect melt temperature and process thermal behavior [49-51]. All the materials used in this study were in pellet form but there were slight differences in their shape and size. The highest difference in the maximum melt temperatures (i.e. among the three materials at the same speed) was observed at 10rpm between LDPE and PP as 3.5^{o}C. Therefore, results show that the nature of the melt temperature profiles differs depending on the material and this has been shown by the previous work as well [6, 44]. There are shoulder regions, but significantly lower temperature regions were not observed in the melt temperature profiles of any material as the BF screw was used for all the experimental trials. Furthermore, it is noticeable that the temperature of the melt at the middle of the flow increased with screw speed for all polymer types investigated.

Effects of barrel set temperature on melt flow temperature homogeneity

Three experimental trials were carried out with the GC screw and RHDPE under three different barrel set temperature conditions (A, B and C) with TCM-6 (i.e. under the EXP-3 and details are given in Table 5). Corresponding melt temperature profiles are shown in Figure 7. Figure legends included at the top of each sub-figure in the format of set temperature condition-screw speed (e.g. A-10 denotes set temperature condition A at 10rpm). The three columns of Figure 7 from left to right show melt temperature profiles with set temperature conditions A, B and C, respectively. The minimum, mean and maximum melt temperatures achieved at each screw speed with different barrel set temperature conditions are given in Table 8. Tests were carried out only at speeds of 10rpm, 50rpm and 90rpm under the set temperature conditions A and C. Also, the data at 90rpm in set temperature condition A is missing as one of the mesh junctions was damaged during the experiment at this screw speed.

It is apparent that higher set barrel temperature resulted in higher mean melt temperature at a particular set screw rotation speed. Slight differences in the shape of the melt temperature profiles were observed at different barrel set temperatures at the same screw speed and similar observations have been reported in the literature [52]. Temperature of the melt in the middle of the flow increased with the screw speed while low temperature shoulder regions were noticeable at high screw speeds. Crabtree et al. [53] observed the effects of barrel set temperatures on the level of melt temperature and mass throughput and similar observations to this study were made. Overall, these results emphasize the importance of the selection of appropriate process settings to achieve the desired melt quality for a given machine and material.

Comparison of thermal fluctuations

The above thermal information relating to the different screws, materials and processing conditions were further analyzed to obtain the level of radial temperature variation across the melt flow (ΔT) and the temporal fluctuations across the melt flow cross-section with reference to the mean temperature (i.e. the standard deviation of melt temperature across the melt flow ($Temp\text{-}SD_{avg}$)) at each screw speed. The melt temperature data collected over the last minute of each screw speed which was used for calculating the T_{mean} was used for this evaluation as well. The minimum and maximum melt temperatures of each radial position over the last minute were obtained and then the difference between the highest and lowest of these values were taken as the ΔT. Likewise, the standard deviation of melt temperature measured at each radial position over one minute (i.e. the data of the last minute at each condition) was calculated and then by taking the average of these values $Temp\text{-}SD_{avg}$ was obtained. In addition to the melt temperature details, melt pressure variation (ΔP) at each screw speed was calculated. Furthermore, mass throughput (*MT*) was measured over the last minute at each screw speed. Graphs corresponding to the T_{mean}, ΔT, $Temp\text{-}SD_{avg}$, ΔP and *MT* are shown in Figure 8. Sub-figures in each row are plotted at the same scale and the details shown in columns 1, 2 and 3 are related to the EXP-1, EXP-2 and EXP-3, respectively (see Table 5).

Each sub-figure of Figure 8 provides a comparison between different screws, materials or processing conditions and the data can be compared with each other to obtain valuable process thermal information. For example, sub-figures 8-(a) and 8-(k) can be compared to explore the effects of the different materials under the same processing conditions (i.e. for LDPE and RHDPE with the GC screw under the set temperature condition B). In general, the mean temperature across the melt flow reduced with increasing screw speed above 50rpm for the GC and RC screws but this is not true for the BF screw. Thermal fluctuations across the melt flow (i.e. ΔT and $Temp\text{-}SD_{avg}$) were much lower with the BF screw compared to other two screws. Moreover, significant temperature differences across the melt flow were observed with the GC and RC screws at high speeds (i.e. around 75^{o}C at 90rpm) and these differences were more than twice the temperature difference generated by the BF screw at the same conditions. Conversely, no significant differences in the mean temperature or temperature fluctuations were seen among polymers under the same processing conditions. However, there were considerable differences in the level of mean temperature across the die melt flow over the different barrel set temperatures as could be expected. Furthermore, melt pressure fluctuations showed a quite similar trend to the thermal fluctuations but only with the BF screw. As was observed during the experiments, mass throughput increased with the screw speed and in a relatively linear fashion for all screws. However, PP was not processed efficiently at set temperature condition B due to the low set barrel temperatures relative to its melting temperature (see Table 3) and hence exhibited low throughputs compared to other two materials. Generally, it is clear that there is a complex relationship between the melt flow thermal behavior in polymer extrusion and the process, material and machine parameters. Clearly, this type of thermal information cannot be observed with the conventional wall mounted thermocouples which are widely used in the current industry. Therefore, it will be highly useful to focus future research to understand the melt flow thermal behavior and also to improve the process thermal monitoring techniques.

CONCLUSIONS & FUTURE WORK

Detailed information on the melt homogeneity of a single screw extruder was obtained using a thermocouple mesh technique. Process thermal homogeneity was significantly affected by screw geometry, material properties and process settings, and melt temperature was found to be highly variable over different processing situations. The relationship between polymer type, extruder screw geometry and process settings was found to be complex in nature leading to a highly variable and unpredictable process. The effect of process settings and screw geometry on melt temperature homogeneity is influenced by factors such as heat generation by conduction and viscous shear, mixing and residence time. Furthermore, each polymer showed considerably different thermal behavior with different screw geometries and process settings. These observations emphasize the importance of appropriate selection of screw geometry and set extrusion conditions for a given polymer to avoid unnecessary thermal fluctuations which can be detrimental to product quality. These results show that the level of the melt temperature significantly varies across the melt flow cross-section and this type of detailed information cannot be obtained from single point measurement techniques commonly used in the polymer processing industry. Thermal profile measurement techniques are not yet industrially available and therefore it is desirable to continue development of suitable robust and non-intrusive techniques.

ACKNOWLEDGEMENTS

This work was supported by Engineering and Physical Sciences Research Council (EPSRC) under grant numbers EP/F021070/1 and EP/G059330/1. The authors would like to thank all who (from Queen's University Belfast and the University of Bradford) supported the research in various ways. Also, the support provided by ‘Cherry Pipes Ltd’ in providing materials is gratefully acknowledged.

REFERENCES

1. J. T. Lindt, Mathematical modelling of melting of polymers in a single screw extruder: A critical review, *Polym. Eng. Sci.*, **25** (10), 585-588, 1985.
2. P. D. Coates, *Measurement & control*, **28**, 1-10, 1995.
3. C. Rauwendaal, Polymer extrusion, 4th Edition, *Hanser-Munich*, 2001.
4. Chamil Abeykoon, Polymer Extrusion: A Study on Thermal Monitoring Techniques and Melting Issues. *Lap Lambert Academic Publishing:Verlag*, 2012.
5. C. Abeykoon, P. J. Martin, A. L. Kelly, E. C. Brown, An evaluation of melt temperature sensors for polymer extrusion, *Sens. Actuators, A*, **182**, 16-27, 2012.
6. Chamil Abeykoon, Modelling and control of melt temperature in polymer extrusion. Ph.D. thesis, Queen's University Belfast, United Kingdom, 2011.
7. B. H. Maddock, Measurement and analysis of extruder stability, *SPE Journal*, **20**, 1277-1283, 1964.
8. E. L. Steward, Recording pressure and melt temperature in extrusion, *Conf. Proc. SPE ANTEC*, **1**, pp 320-324, 1998.
9. E. L. Steward, Control of melt temperature on single screw extruders, *Conf. Proc. SPE ANTEC*, **1**, Paper No: 813, 1999.
10. X. Shen, R. Malloy, and J. Pacini, An experimental evaluation of melt temperature sensors for thermoplastic extrusion, *Conf. Proc. SPE ANTEC*, 918-926, 1992.
11. V. Schoppner, E. Enns, K. Anger, and E. Giese, Dynamic temperature measurement in polymer processing, *Conf. Proc. SPE ANTEC*, 228-232, 2008.
12. C. Warren, IR sensors: A good approach for industrial and process applications, *Chilton's instruments and control*, **58** (6), 36-38, 1985.
13. C. Maier, Infrared temperature measurement of polymers, *Polym. Eng. Sci.*, **36** (11), 1502-1512, 1996.
14. W. Obendrauf, G. R. Lagecker, W. Friesenbichler, Temperature measuring in plastics processing with infrared radiation thermometers, *Int. Polym. Proc.*, **13** (1), 71-77, 1998.
15. K. D. Sabota, D. R. Lawson, J. S. Huizinga, Advanced temperature measurements in polymer extrusion, *Conf. Proc. SPE ANTEC*, **2**, 2832-2842, 1995.

16. Tzu-Fang Chen, Ky T. Nguyen, Szu-Sheng L. Wen and Cheng-Kuei Jen, Temperature measurement of polymer extrusion by ultrasonic techniques, *Meas. Sci. Technol.*, **10** (3), 139-145, 1999

17. E. C. Brown, P. Olley, P. D. Coates, In line melt temperature measurement during real time ultrasound monitoring of single screw extrusion, *Plast. Rubber Compos.*, **29** (1), 3-13, 2000.

18. E. C. Brown, A. L. Kelly, P. D. Coates, Melt temperature homogeneity in single screw extrusion: effect of material type and screw geometry, *Conf. Proc. SPE ANTEC*, **1**, 183-187, 2004.

19. J. Muller, S. Kummer, D. Fischer, New ultrasonic probes for in-line monitoring of polymer melts, *Meas. Sci. Technol.*, **20** (9), 1-4, 2009.

20. E. C. Brown, T. L. D Collins, A. J. Dawson, P. Olley, P.D. Coates, Ultrasound: A virtual instrument approach for monitoring of polymer melt variables, *J. Reinf. Plast. Compos.*, **18** (4), 331-338, 1999.

21. K. Trivedi, D. Cuff, C. L. Thomas, In-Process temperature measurement in extrusion using continuous wave ultarsound, *Conf. Proc. SPE ANTEC*, **1**, 1271-1273, 2004.

22. S. S. L. Wen, T. F. Chen, D. R. Franca, K. T. Nguyen, C. K. Jen, I. Ihara, A. Derdouri, A. G. Rejon, Resent progress in on-line ultrasonic process monitoring, *Proc. Int. Soc. Opt. Eng.*, **3399**, 122-131, 1998.

23. A. Bendada and M. Lamontagne, A new infrared pyrometer for polymer temperature measurement during extrusion molding, *Infrared Phys. Technol.*, **46** (1-2), 11-15, 2004.

24. A. W. Christie, Using thermal process imaging for extruder analysis and improvement, *Conf. Proc. SPE ANTEC*, **1**, 335-339, 2005.

25. R. Spares, B. R. Whiteside, P. D. Coates, High speed thermal imaging of micromoulding, *Conf. Proc. SPE ANTEC*, 2750-2753, 2009.

26. A. Gottwald, U. Scheler, Extrusion monitoring of polymer melts using a high-temperature surface-NMR probe, *Macromol. Mater. Eng.*, **290** (5), 438-442, 2005.

27. Y. Yang, W. Yang, H. Zoang, Temperature distribution measurement and control of extrusion process by tomography, *IEEE International Workshop on Imaging Systems and Techniques* (*IEEE IST*), Chania, Greece, pp 170-174, 2008.

28. W. Schlaffer, J. Schijf, H. Janeschitz-Kriegl, Measurements of radial temperature profiles in a single-screw extruder, *Plast. Polym.*, **39** (141), 193-199, 1971.

29. I. Bruker, C. Miaw, A. Hasson, G. Balch, Numerical analysis of the temperature profile in the melt conveying section of a single screw extruder: Comparison with experimental data, *Polym. Eng. Sci.*, **27** (7), 504-509, 1987.
30. C. Miaw, A. Hasson, G. Balch, Melt temperature measurement in a single screw extruder, *Conf. Proc. SPE ANTEC*, 86-79, 1985.
31. M. Esseghir, V. Sernas, On the measurements of the radial temperature distribution in an extruder channel, Adv. Polym. Tech., **13** (2), 133-140, 1994.
32. C. L. Tucker (Edited by), Fundamentals of computer modeling for polymer processing, *Hanser*, Ch. 6, 1989.
33. A. L. Kelly, E. C. Brown, M. Woodhead, P. D. Coates, Melt temperature field measurement and modelling in extrusion, *Conf. Proc. SPE ANTEC*, **3**, Paper No: 708, 2002.
34. A. J. Bur, S. C. Roth, M. A. Spalding, D. W. Baugh, K. A. Koppi, W. C. Buzanowski, Temperature gradients in the channels of a single-screw extruder, *Polym. Eng. Sci.*, **44** (11), 2148-2157, 2004.
35. E. C. Brown, A. L. Kelly, P. D. Coates, Melt temperature field measurement in single screw extrusion using thermocouple meshes, *Rev. Sci. Instrum.*, **75** (11), 4742–4748, 2004.
36. A. L. Kelly, E. C. Brown, P. D. Coates, Melt temperature field measurement in single screw extrusion: influence of melt pressure and die geometry, *Conf. Proc. SPE ANTEC*, **1**, 291-295, 2005.
37. A. L. Kelly, E. C. Brown, P. D. Coates, The effect of screw geometry on melt temperature profile in single screw extrusion, *Polym. Eng. Sci.*, **46** (12), 1706-1714, 2006.
38. A. L. Kelly, E. C. Brown, K. Howell, P. D. Coates, Melt temperature filled measurement in extrusion using thermocouple meshes, *Plast. Rubber Compos.*, **37** (2-4), 151-157, 2008.
39. C. Abeykoon, M. McAfee, K. Li, A. L. Kelly, E. C. Brown, Monitoring the effect of operating conditions on melt temperature homogeneity in single-screw extrusion, *Conf. Proc. SPE ANTEC*, **1**, 1799-1806, 2010.
40. C. Abeykoon, K. Li, M. McAfee, P. J. Martin, J. Deng, A. L. Kelly, Modeling the effects of operating conditions on die melt temperature homogeneity in single screw extrusion, *UKACC Int. Conf. on Control*, Coventry, UK, pp 42-47, 2010.
41. C. Abeykoon, K. Li, M. McAfee, P. J. Martin, Q. Niu, A. L. Kelly, J. Deng, A new model based approach for the prediction and optimization of thermal homogeneity in single screw extrusion, *Control Eng. Pract.*, **19** (8), 862-874, 2011.

42. C. Abeykoon, M. McAfee, K. Li, P. J. Martin and A. L. Kelly, The inferential monitoring of screw load torque to predict process fluctuations in polymer extrusion, *J. Mater. Process. Technol.*, **211** (12), 1907-1918, 2011.

43. C. Abeykoon, K. Li, P. J. Martin, A. L. Kelly, Monitoring and modeling of the effects of process settings and screw geometry on melt pressure generation in polymer extrusion, *Int.J. of Syst. Control and Inf. Process.*, **1** (1), 71-88, 2012.

44. A. L. Kelly, E. C. Brown, and P. D. Coates, Melt temperature field measurement: influence of extruder screw and die geometry, *Plast. Rubber Compos.*, **34** (9), 410-416, 2005.

45. J. A. Myers and R. A. Barr, Improved screw design for maximum conductive melting, *Conf. Proc. SPE ANTEC*, 2002.

46. A. Altinkaynak , M. Gupta, M. A. Spalding and S. L. Crabtree, Numerical investigation of the effect of screw temperature on the melting profile in a single-screw extruder, *Conf. Proc. SPE ANTEC*, 430-434, 2007.

47. E. M. Mount, Evaluation of the melting capacity of three single screws, *Conf. Proc. SPE ANTEC*, 400-404, 2007.

48. G. P. Colbert, Time uniformity of extrudate melt temperature*, Rubber World*, **202** (4), 27-31, 1990.

49. S. J. Derezinski, Dynamic torque of a single screw extruder, *Conf. Proc. SPE ANTEC*, Vol. 1, Paper # 113, 2001.

50. D. S. Kim, B. K. Lee, H. S. Kim, J. W. Lee and C. G. Gogos, A study of size and frictional effects on the evolution of melting Part I: Batch mixer, *Korea-Australia Rheology Journal*, 11 (1), 44-49, 1999.

51. D. S. Kim, B. K. Lee, H. S. Kim, J. W. Lee and C. G. Gogos, A study of size and frictional effects on the evolution of melting Part II: Twin screw extruder, *Korea-Australia Rheology Journal*, 13 (2), 89-95, 2001.

52. R. Rasid, and A. K. Wood, Effect of process variables on melt velocity profiles in extrusion process using single screw plastics extruder. *Plast. Rubber Compos.*, **32** (5), 193–198, 2003.

53. S. L. Crabtree, M. A. Spalding, and C. L. Pavlicek, Single-screw extruder zone temperature selection for optimized performance, *Conf. Proc. SPE ANTEC*, 1410-1415, 2008.

Key Words: Polymer Extrusion, Thermal Monitoring, Melt Temperature Homogeneity, Melt Temperature Profile, Process Settings, Screw Geometry, Materials.

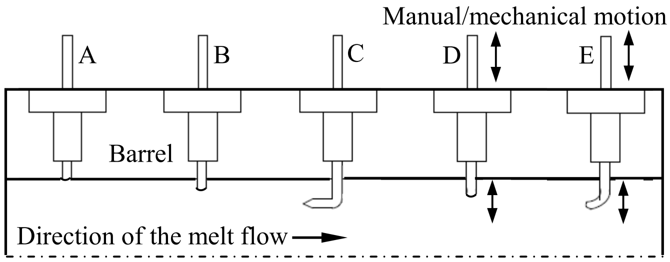

Figure 1: Possible ways of contact of the wall mounted thermocouple probes with the melt flow, A – Flush mounted probe, B and C - Intrusive probe, D and E – Traversing probe

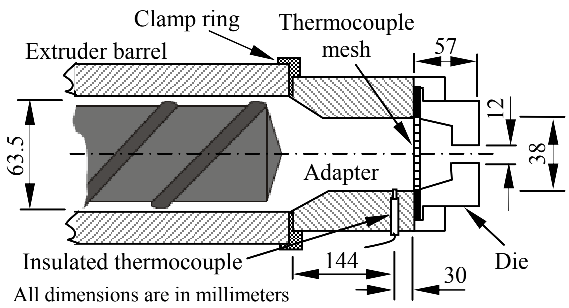

Fig. 2: Arrangement and dimensions of the apparatus

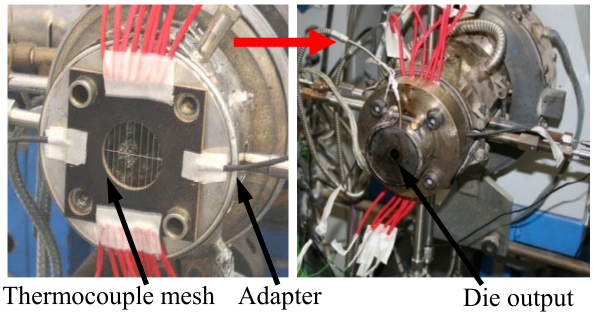

Fig. 3: Extruder die, adapter, and thermocouple mesh

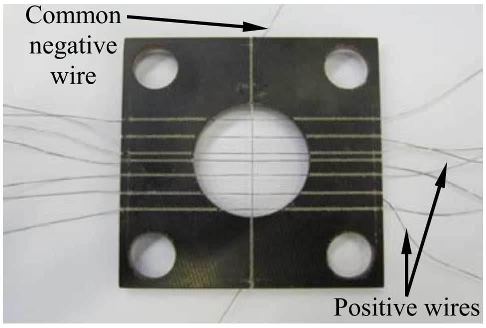

Fig. 4: The physical arrangement of a thermocouple mesh

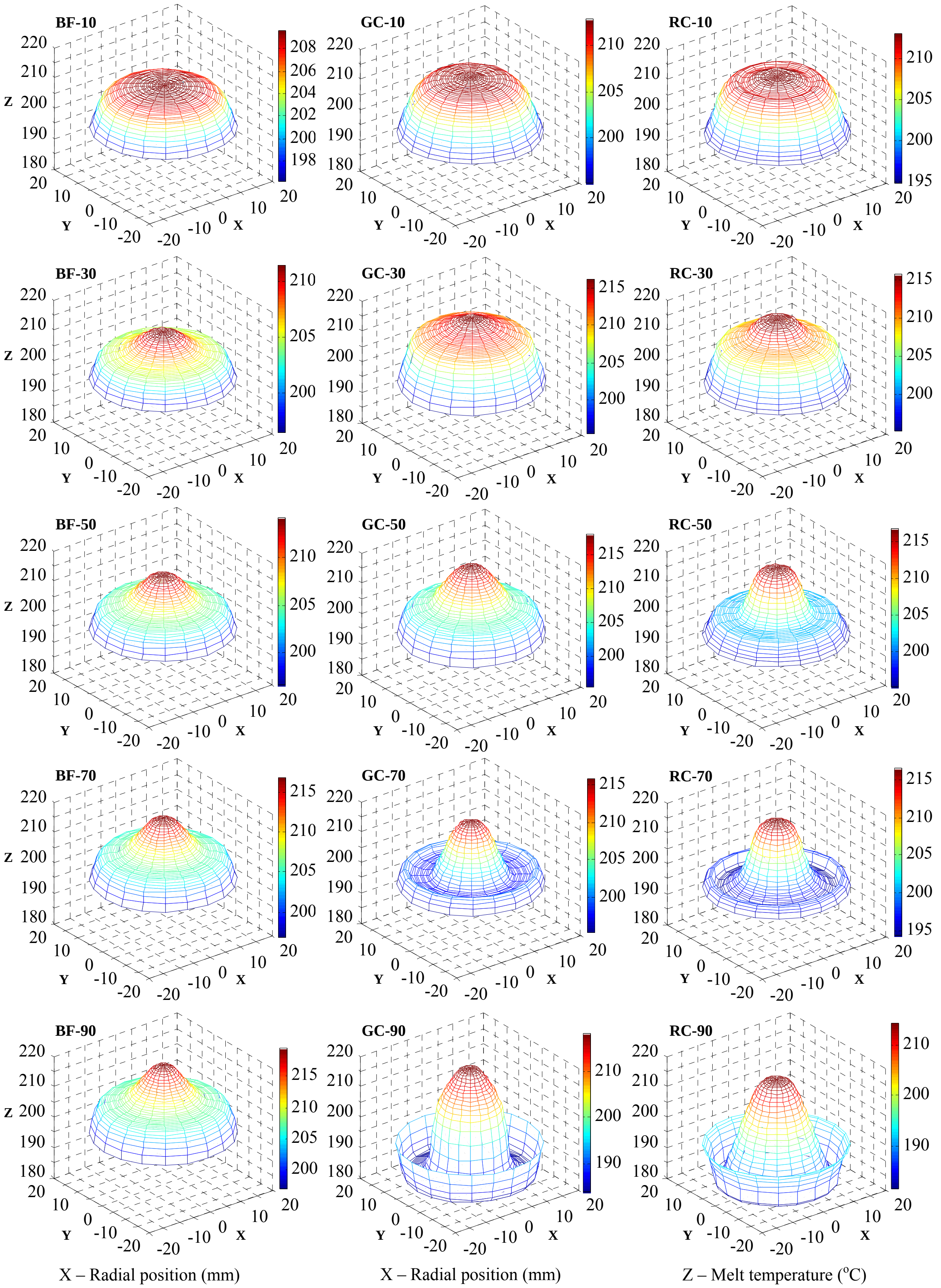

Figure 5: Temperature profiles of the melt flow with the BF, GC and RC screws at different screw speeds with LDPE material

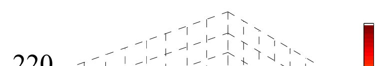

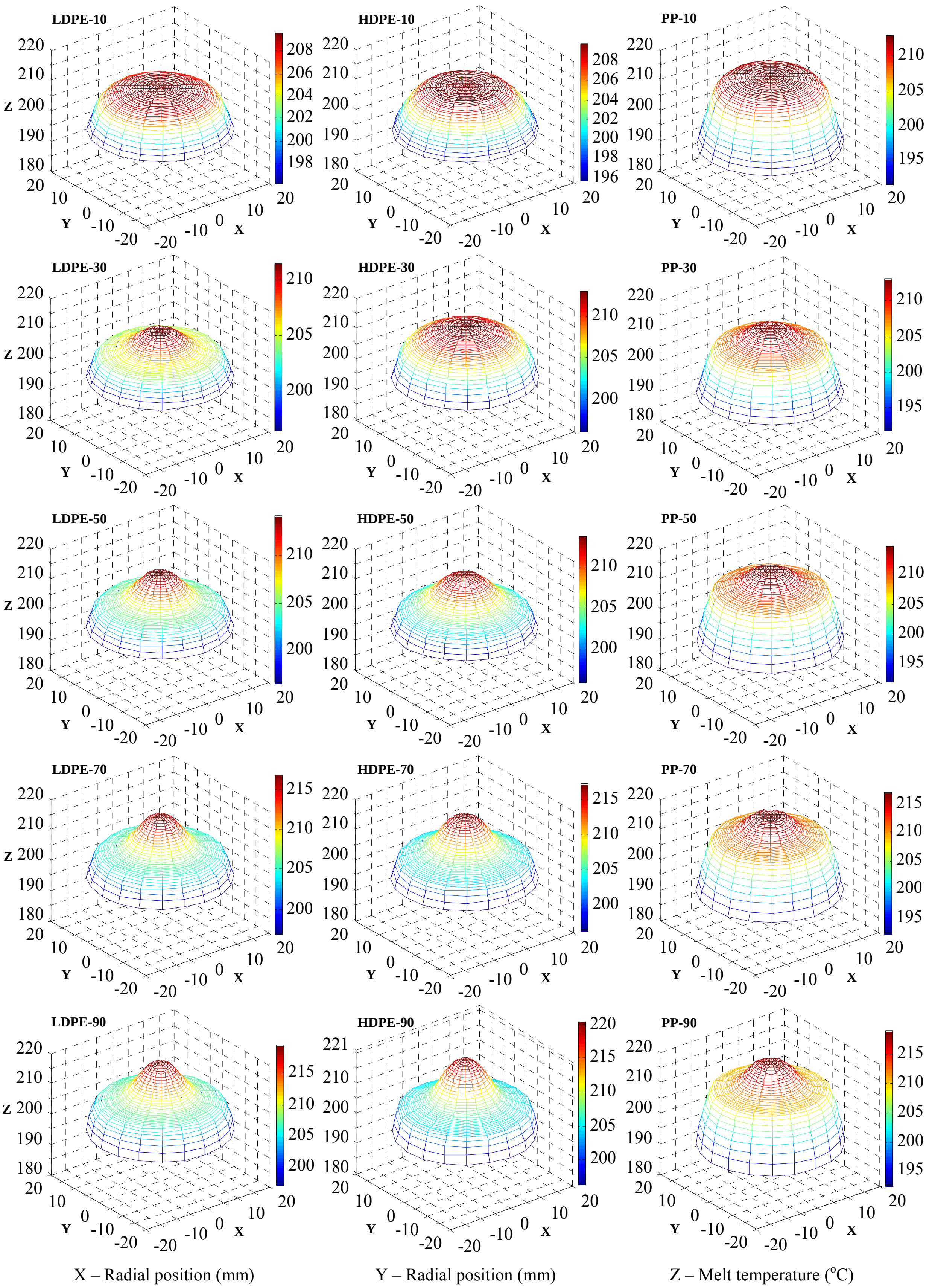

Figure 6: Temperature profiles of the melt flow of LDPE, HDPE and PP materials at different screw speeds with the BF screw

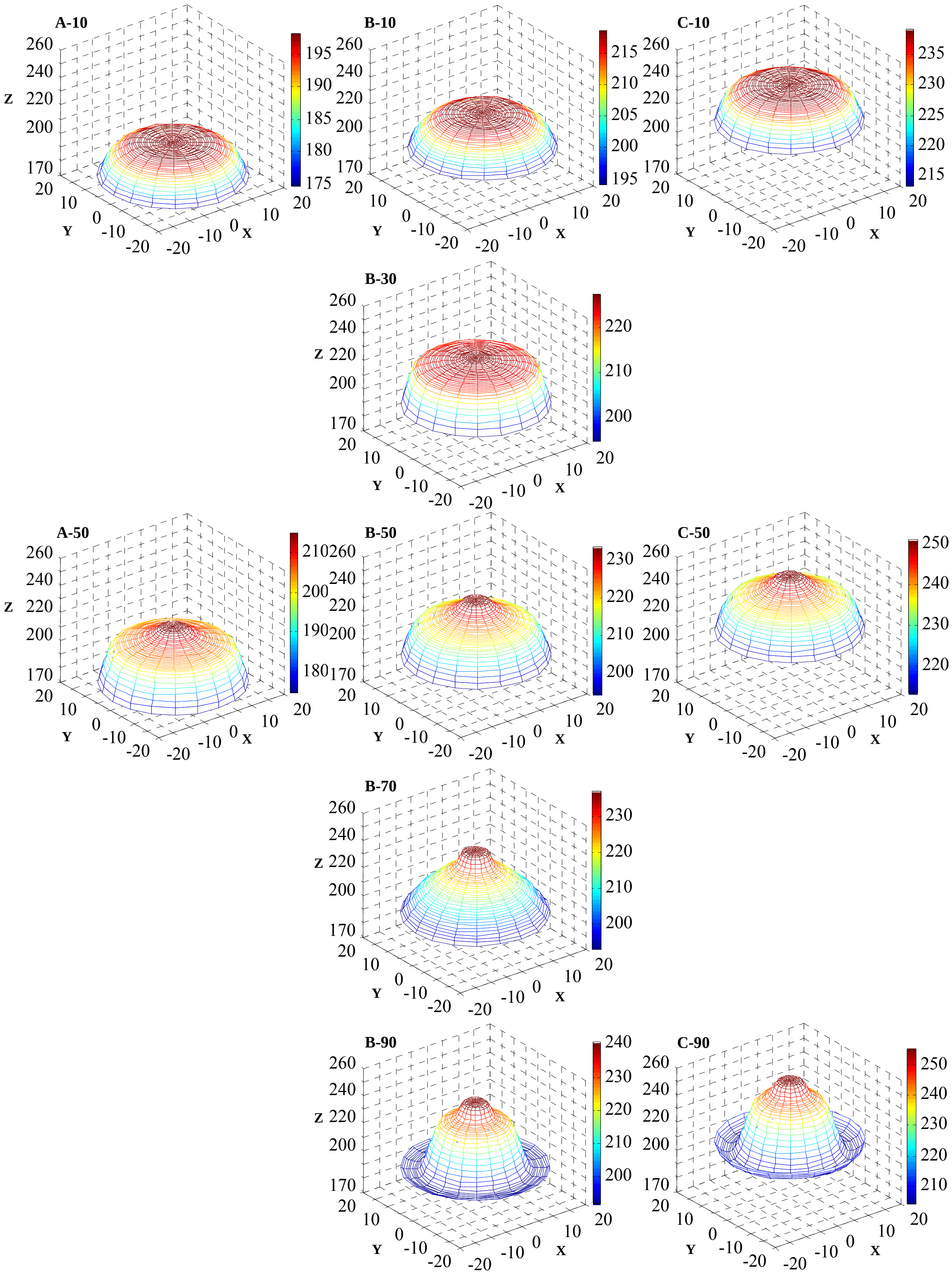

X – Radial position (mm)   Y – Radial position (mm)   Z – Melt temperature (°C)

Figure 7: Temperature profiles of the melt flow of RHDPE material at different screw speeds and barrel set temperature conditions

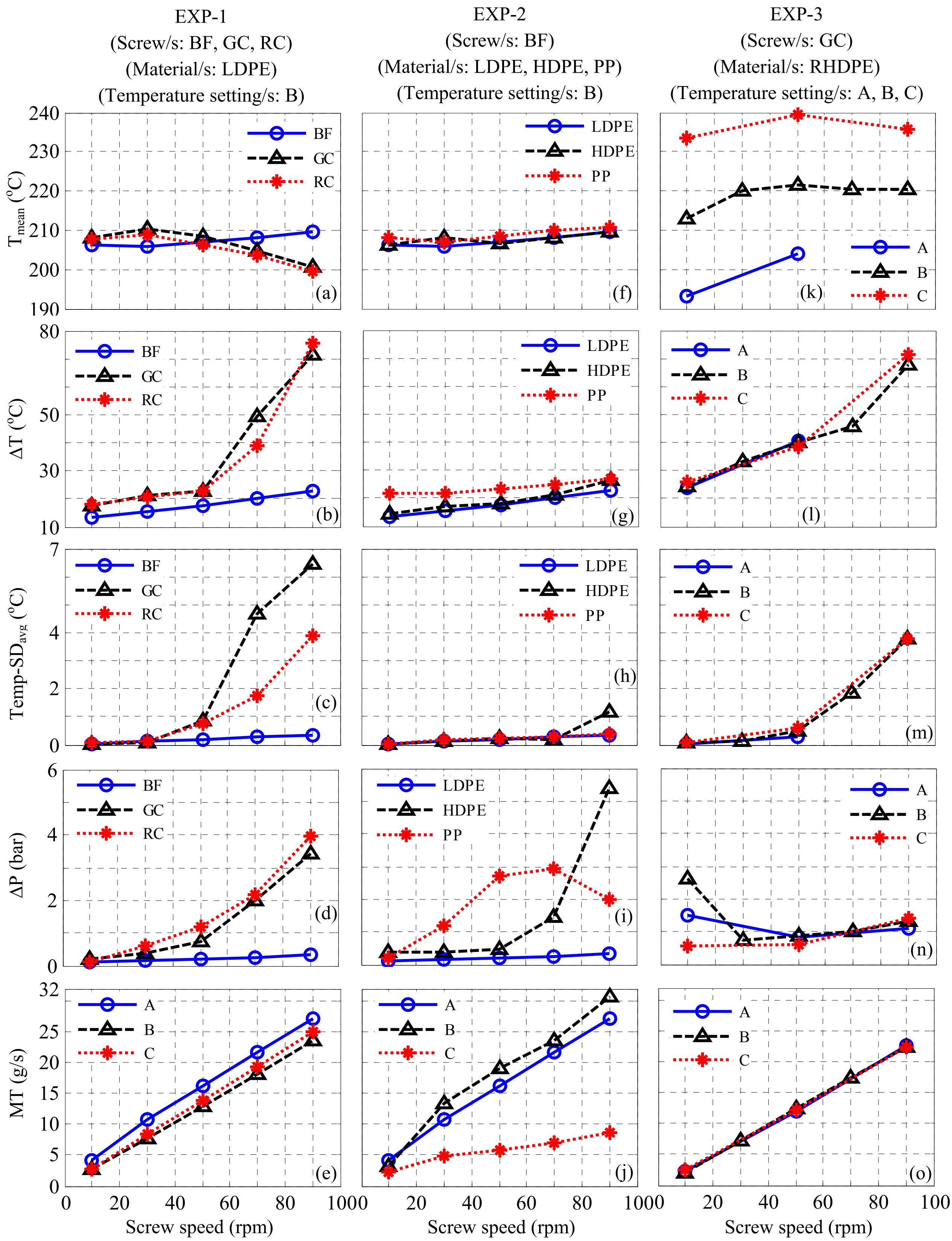

Fig. 8: Thermal information across the melt flow with the different screws, materials and barrel set temperature conditions

Table. 1: Geometrical details of the screws used for experiments

Screw	CR	Feed		Melting	Metering	
		L	H (mm)	L	L	H (mm)
GC	3:1	4D	10.53	10D	10D	3.46
RC	3:1	12D	10.53	2D	10D	3.50
BF	2.5:1	5D	12.19	13D	6D	4.90

Table. 2: Details of the thermocouple mesh used for experiments

TCM	Distance to the each mesh junction from die centre (mm)	Number of junctions
1	0, −3.5, +4.5, +9.2, +10.5, −15.8, +16.5	7
2	0, −2.5, +4.3, +8.5, +11.0, −15.0, +16.8	7
3	0, −3.5, +4.0, +9.5, +11.0, −15.5, +17.5	7
4	0, −3.0, +4.3, +9.0, +11.0, −15.0, +17.0	7
5	0, −2.5, +3.5, +9.0, +11.3, −14.5, +16.7	7
6	0, −3.0, +5.0, −8.5, −15.0	5
7	0, +2.4, −5.4, +7.6, −11.2, −17.0	6
8	0, +3.0, −4.5, +8.8, −11.0, +14.7, −16.5	7

Table. 3: Details of the materials used for experiments

Material	Density (g/cm^3)	Melt flow index (g/10min)	Melting temperature (°C)	Resin form
HDPE	0.952	0.12 (@ 190°C, 2.16kg)	134	Pellets
RHDPE	0.967	0.16 (@ 190°C, 2.16kg)	130-132	Pellets: contains ~2.5% carbon black by weight
LDPE	0.921	0.25 (@ 190°C, 2.16kg)	111	Pellets
PP	0.952	3.00 (@ 230°C, 2.16kg)	163	Pellets

Table. 4: Extruder barrel temperature settings

Test	Temperature settings (^oC)						
	Barrel zones				Clamp ring	Adapter	Die
	1	2	3	4			
A	130	155	170	180	180	180	18
B	140	170	185	200	200	200	20
C	150	185	200	220	220	220	22

Table. 5: Details of the experiments

Experiment	Screw	Temperature settings	Materials	Speed (rpm)	
				Range	Steps
EXP-1	GC, RC, BF	B	LDPE	0-90	20
EXP-2	BF	B	LDPE, HDPE, PP	0-90	20
EXP-3	GC	A, B, C	RHDPE	0-90	20, 40

Table 6: Minimum (Min), mean and maximum (Max) temperatures of the melt flow at each speed with m different screw geometries

Screw	Min., Mean and Max. temperatures at each screw speed (^{o}C)														
	10rpm			30rpm			50rpm			70rpm			90rpm		
	Min	Mean	Max	Min	Mean	Max	Min	Mean	Max	Min	Mean	Max	Min	Mean	Max
BF	196.3	206.2	209.6	196.4	205.9	211.5	196.6	206.8	214.1	196.9	208.2	216.9	197.2	209.8	219.4
GC	195.1	208.0	212.8	195.5	210.2	216.3	195.5	208.6	217.8	195.5	204.6	215.9	183.6	200.6	218.1
RC	194.8	207.9	213.1	195.2	208.8	215.6	195.1	206.2	216.8	194.3	203.6	216.4	181.6	199.4	214.4

Table 7: Minimum, mean and maximum temperatures of each material at different speeds

Material	Min., Mean and Max. temperatures at each screw speed (^oC)														
	10rpm			30rpm			50rpm			70rpm			90rpm		
	Min	Mean	Max	Min	Mean	Max	Min	Mean	Max	Min	Mean	Max	Min	Mean	Max
LDPE	196.3	206.2	209.6	196.4	205.9	211.5	196.6	206.8	214.1	196.9	208.2	216.9	197.2	209.8	219.4
HDPE	195.7	206.1	209.9	196.2	208.2	213.0	196.1	206.7	213.8	196.3	208.1	217.1	196.4	209.7	220.5
PP	191.6	208.0	213.1	191.8	206.9	213.1	192.0	208.5	214.8	192.3	209.8	216.9	192.5	210.7	218.8

Table 8: Minimum, mean and maximum temperatures at each speed with different set temperature conditions

Set temperature condition	Min., Mean and Max. temperatures at each screw speed (^oC)														
	10rpm			30rpm			50rpm			70rpm			90rpm		
	Min	Mean	Max	Min	Mean	Max	Min	Mean	Max	Min	Mean	Max	Min	Mean	Max
A	174.8	193.1	198.5	-	-	-	175.0	204.0	215.4	-	-	-	-	-	-
B	194.2	212.9	218.8	194.6	220.2	227.8	194.0	221.4	234.2	192.7	220.3	238.5	176.3	220.4	244.0
C	213.4	233.5	239.2	-		-	213.0	239.4	251.7	-		-	188.5	235.7	260.0